



LAWRENCE
LIVERMORE
NATIONAL
LABORATORY

Understanding the stagnation and burn of implosions on NIF

J. Kilkenny, J. A. Caggiano, J. P. Knauer, B. K. Spears, J. Cerjan, L. Divol, M. Eckart, R. Hatarik, H. Herrmann, S. Le Pape, D. Munro, D. B. Sayre, S. V. Weber, C. B. Yeamans, G. Grim, O. S. Jones, L. Berzak Hopkins, M. Gatu-Johnson, A. Mackinnon, N. Meezan, D. Casey, J. Frenje, J. Mcnaney, R. Petrasso, A. Zylstra, H. Rinderknecht

October 31, 2013

8th International Conference on Inertial Fusion Sciences and
Applications
Nara, Japan
September 8, 2013 through September 13, 2013

Disclaimer

This document was prepared as an account of work sponsored by an agency of the United States government. Neither the United States government nor Lawrence Livermore National Security, LLC, nor any of their employees makes any warranty, expressed or implied, or assumes any legal liability or responsibility for the accuracy, completeness, or usefulness of any information, apparatus, product, or process disclosed, or represents that its use would not infringe privately owned rights. Reference herein to any specific commercial product, process, or service by trade name, trademark, manufacturer, or otherwise does not necessarily constitute or imply its endorsement, recommendation, or favoring by the United States government or Lawrence Livermore National Security, LLC. The views and opinions of authors expressed herein do not necessarily state or reflect those of the United States government or Lawrence Livermore National Security, LLC, and shall not be used for advertising or product endorsement purposes.

Understanding the stagnation and burn of implosions on NIF

J. D. Kilkenny⁵, J. A. Caggiano¹, J. P. Knauer², B. K. Spears¹, J. Cerjan¹, L. Divol¹, M. Eckart¹, R. Hatarik¹, H Herrmann³, S. Le Pape¹, D. Munro¹, D. B. Sayre¹, S.V. Weber¹, C B Yeamans¹, G. Grim³, O. S. Jones¹, L. Berzak Hopkins¹, M. Gatu-Johnson⁴, A. Mackinnon¹, N. Meezan¹, D. Casey¹, J. Frenje⁴, J. Mcnaney¹, R. Petrasso⁴, A. Zylstra⁴, H. Rinderknecht⁴

¹Lawrence Livermore National Laboratory, 7000 East Ave., Livermore, CA 94550 USA

²Laboratory for Laser Energetics, Univ. of Rochester, Rochester, New York 14623, USA

³Los Alamos National Laboratory, Los Alamos, NM 87545, USA

⁴Plasma Science and Fusion Center, Massachusetts Institute of Technology, Cambridge, Massachusetts 02139, USA

⁵General Atomics, 3550 General Atomics Court, San Diego, CA, 29186, USA

Abstract

An improved set of nuclear diagnostics on NIF measures the properties of the stagnation plasma, including the drift velocity, β anisotropy, and carbon β in the compressed core. Two types of deuterium-tritium (DT) gas-filled targets are imploded by shaped x-ray pulses that produce stagnated and burning DT cores of radial convergence (C_r) ~ 4 and ~ 20 . Comparison with two-dimensional modeling with inner and outer surface mix shows good agreement with an x-ray drive that is reduced to match the measured implosion dynamics.

1 Introduction

The indirect drive inertial confinement fusion approach at the National Ignition Facility (NIF) uses x-rays to ablatively drive the implosion of a spherical shell at the center of the hohlraum. The shell has a multi-layered ablator. The radiation drive is shaped to launch 3-4 staged shocks to control the adiabat and to achieve high compression of the cryogenically layered fuel (1). For low-foot designs the measured capsule yield is substantially lower than simulations (2). It has been known for decades, based on theory (3) and experiments with high-power lasers, (4,5) that implosions are doubly unstable to the Rayleigh-Taylor (RT) instability, which can lead to ablator material contaminating the hot spot and quenching the burn. In an effort to understand the DT burn discrepancy, gas-filled plastic capsules are imploded as simulants of cryogenically layered implosions that are in an “ignition” hohlraum with an ignition pulse shape (1). The gas fill results in a lower convergence, less stressing implosions. Improved nuclear diagnostics measure the drift velocities and areal densities of the imploded cores as well as the normal attributes: yield, ion temperature, down scattered fraction, etc. There is good agreement with 2D simulations.

2 Gas Filled Implosions to Emulate Layered Implosions

Two types of gas-filled implosions are discussed here. The first is a high-yield x-ray drive “exploding pusher.” The goal was to get low areal density implosion with a good yield and low-drift velocity. This is satisfied by a single shock, $C_r \sim 4$ x-ray driven implosion (6). These experiments produced well understood stagnation plasma to test the upgraded diagnostics of section 3. The second type is a set of higher convergence, $C_r \sim 20$ and more stressing implosions. The design consists of four shocks and a target as with the layered implosions (1), but with a thicker plastic shell to emulate the DT ice and a gas fill.

Simulations of these experiments represent the conditions of an actual experiment, including the as-shot capsule metrology, capsule surface roughness, and the tent (the thin foils that hold the capsule in the hohlraum) as seeds for the growth of hydrodynamic instabilities. The 2D zoning resolves up to $l=100$. The radiation drive used in these capsule-only simulations is reduced to match the measured implosion timing, kinematics, and low-mode asymmetry. These simulations follow reference (2) and have a mix prescription for the inner surface as it is decelerated by the gas, representing $0.05 \times$ the distance to the fall line. The fall-line fraction is a simple parameterized prescription to introduce time dependent mix based on the Read and Youngs' (7) mix measurements. A fall-line mix parameter of 0.05 was chosen to match more sophisticated modeling.

3 The improved set of neutron diagnostics

Recent upgrades to NIF's nuclear diagnostics allow better measurements of the properties of the stagnating and burning compressed core. The augmented nuclear diagnostic suite was validated on the $C_r \sim 4$ implosions and then used on $C_r \sim 20$ implosions.

3a: Neutron Time of Flight (nToF) detectors: The initial set of NIF diagnostic had two spectrally resolving nToF (8) with a 20-m flight path. A recent additional 18-m distance nToF near the south pole of the chamber gives three close-to-orthogonal views with spectrally resolving detectors. Modifications to the original design use a faster scintillator (9), have lower neutron scattering, a faster scintillator, and faster recording. These improvements allow measurements of the drift velocity and carbon scattering edges (10) to be made. These nToF measure yield, ion temperature T_{ion} , and down-scattered neutrons as described in ref 11. Additionally, if the neutron-emitting imploded core has an average drift velocity toward a detector, it will slightly increase the neutron velocity in the laboratory frame, resulting in an earlier arrival. To demonstrate the ability to measure drift velocities, three shots were performed with a symmetric drive, a 4% upwards, and 4% downwards drive asymmetry.

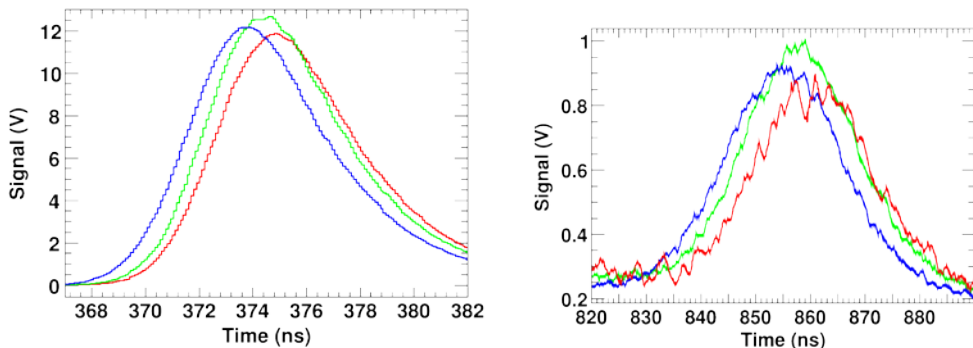


Figure 1: nToF signals near the south pole for DT neutrons (left) and DD neutrons (right). The blue trace is for a deliberate downwards P_1 drive of 4%, the green trace is for a symmetric drive, and the red trace is for a deliberate upwards P_1 drive of 4%. Drift velocities are obtained by fits to the data with a fitting error equivalent to ~ 10 km/s. For the DT and DD neutrons, the drift velocities in km/s are 76, 1, and -76 and 62, -12 and -78 respectively.

The nToF traces for both the DT neutrons and the DD neutrons are shown in Figure 1. To calculate the drift velocities the bang time, when the neutrons are generated by the implosion they are measured by time-resolved x-ray emission and neutron emission to an accuracy of about 100 psec. The velocity of the neutron in the lab frame uses the measured T_{ion} (12). The drift velocities as seen by the shifts in arrival time for both the DD and the DT neutrons agree and reverse as expected with

the imposed asymmetry. The differences between the DD and DT velocities can be as great as 20 km/s : this difference is under investigation.

3b: Flange Neutron Activation Diagnostic System (FnADS): The FnADS system on NIF (13) uses $^{90}\text{Zr} (n,2n)^{89}\text{Zr}$ activation measured by zirconium (Zr) slugs mounted in up to 19 flange covers on the NIF target chamber. Measured activation anisotropy can be due to anisotropy in the flux of un-scattered neutrons or a drift velocity. The variation in the activation for the deliberately P_1 upward and downward drive asymmetry is shown in Figure 2 indicating an increase in activation in the direction of motion. If the measured velocities are used to correct the anisotropy in yield, the remaining anisotropy due to areal density variations is obtained. Some level of consistency with the down-scattered ratio is obtained.

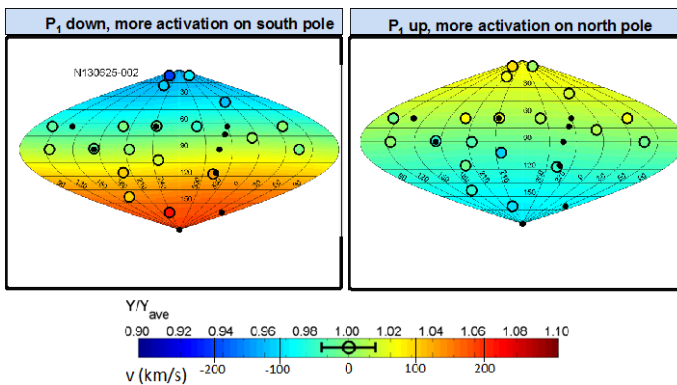


Figure 2: The variation in activation for the experiment in which a deliberate downward (left) and upward (right) P_1 drive asymmetry was imposed.

3c: The Gamma Reaction History (GRH) detector: The GRH diagnostic measures the 4.4 MeV gamma line from the $^{12}\text{C}(n,n'\gamma)$ reaction(14). The GRH was absolutely calibrated by measuring the 4.4 MeV line emitted from a puck of carbon held 1 cm from a calibrated exploding pusher target. On the implosions described here, the carbon that is close to the neutron emitting core at bang time emits 4.4 MeV from $^{12}\text{C}(n,n'\gamma)$ excitation, measuring the ^{12}C pr. Figure 3 shows the good agreement between measured and calculated gamma yields for the single shock (bottom left) and four shock implosions (top right).

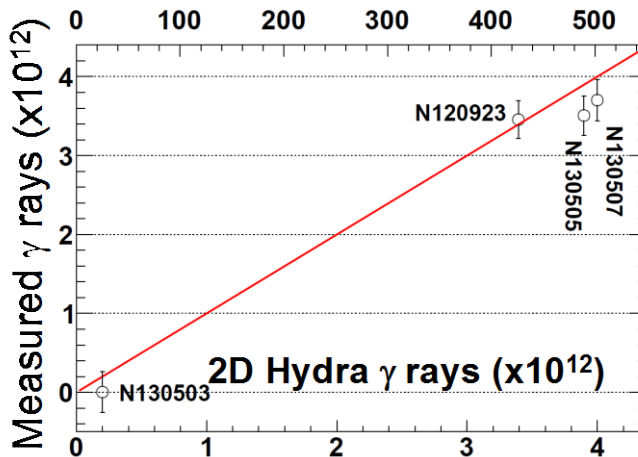


Figure 3: Measured and calculated 4.4 MeV gamma yields from GRH. The upper horizontal axis is the calculated ^{12}C ρr (mgm/cm²).

4 Comparison of experiments with simulations

The DD and DT yields are compared to simulations in Figure 4 and show excellent agreement for the one-shock implosions and good agreement (80%) for the four-shock system. T_{ion} from DD and DT burn are also compared to simulations in Figure 4. There is excellent agreement with the simulations. As expected, from the stronger dependence on T_{ion} for the DT reaction, the time and spatial averaged T_{ion} is larger for the DT reaction than from the DD reaction by about 200 eV as expected.

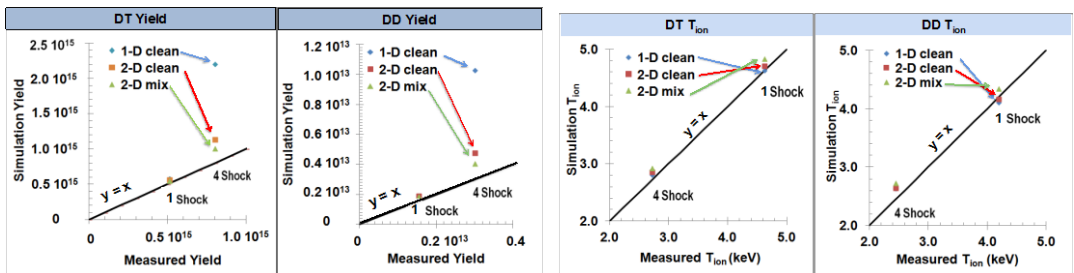


Figure 4: Calculated and measured DT and DD neutron yield (left) and corresponding T_{ions} for the one and four shock systems.

This work was performed under the auspices of the U.S. Department of Energy by Lawrence Livermore National Laboratory under Contract DE-AC52-07NA27344.

References

- (1) M. J. Edwards et. al., Phys. of Plasmas **20**, 070501 (2012)
- (2) D. S. Clark et. al. Phys. of Plasmas **20**, 056318 (2013)
- (3) J.D. Lindl and W.C. Mead, "Two-dimensional simulation of fluid instability in laser-fusion pellets," PPhys. Rev. Lett. 34, 1273 (1975).
- (4) J.S. Wark, J.D. Kilkenny, A.J. Cole, M.H. Key, and P. T. Rumsby, "Observations of the Rayleigh-Taylor instability in laser imploded microballoons," Appl. Phys. Lett. 48, 969 (1987).
- (5) J. D. Kilkenny, "Experimental results on hydrodynamic instabilities in laser-accelerated planar packages," Phys. Fluids B **2**, 1400 (1990).
- (6) S. LePape, submitted to Phys Rev. Lett.
- (7) K. I. Read, 1984 *Physica D* 12, 45. Youngs, D. L. 1984 *Physica D* 12, 32.
- (8) V. Glebov, et. al., Rev. Sci. Instrumen. **81**,10D325(2010)
- (9) R. Hatarik et. al., Rev. Sci. Instrumen. **83**, 10D911 (2012)
- (10) C. J. Forrest et. al., Rev. Sci. Instrumen. **83**, 10D919 (2012)
- (11) R. Lerche, Rev. Sci. Instrumen. **81**, 10D319 (2010)
- (12) L. Ballabio, J. Kallne , G. Gorini Nuclear Fusion, **38**, 1723 (1999)
- (13) C. B., Yeamens et. al. Rev. Sci. Instrumen. **83**,10D313 (2012)
- (14) D. B. Sayre et. al. , Rev. Sci. Instrumen. **83**, 10D905 (2012).